ARTICLE
Journal of Cellular Biochemistry 118:2615–2624 (2017)

Journal of Cellular Biochemistry

Inhibition of the PI3K/AKT Pathway Sensitizes Oral Squamous Cell Carcinoma Cells to Anthracycline-Based Chemotherapy In Vitro

Dmitriy Smolensky,[1,2] Kusum Rathore,[2] Jennifer Bourn,[1,2] and Maria Cekanova[1,2]*

[1]*UT-ORNL Graduate School of Genome Science and Technology, University of Tennessee, Knoxville 37996, Tennessee*

[2]*Department of Small Animal Clinical Sciences, College of Veterinary Medicine, University of Tennessee, Knoxville 37996, Tennessee*

ABSTRACT

Anthracycline-based chemotherapy, such as doxorubicin (Dox), while effective against many solid tumors, is not widely used for head and neck cancers. In this study, we evaluated the efficacy of Dox, and its derivative AD198 in human, canine, and feline oral squamous cell carcinomas cells (OSCC) in vitro. Dox and AD198 had significant an anti-proliferative effect on human, canine, and feline OSCC cells in dose-dependent manner. AD198 inhibited cell proliferation more effectively than Dox in tested OSCC cells. In the human oral squamous cell carcinoma SCC25 cells, Dox and AD198 increased the production of reactive oxygen species and subsequently increased apoptosis through activation of caspase signaling pathway. Dox and AD198 increased activation of AKT, ERK1/2, and p38 MAPK signaling pathways in tested OSCC cells by dose-dependent manner. The efficacy of Dox and AD198 treatments in inhibition of cell proliferation was increased in tested OSCC when combined with PI3K/AKT inhibitor, LY294002 treatment. Inhibition of PI3K/AKT reduced Dox- and AD198-induced activation of ERK1/2 and further increased Dox- and AD198-induced phosphorylation of p38 MAPK in OSCC. Our results suggest that the anthracycline therapies, such as Dox or AD198, can be more effective for treatment of OSCC when combined with inhibitors of the PI3K/AKT pathway. J. Cell. Biochem. 118: 2615–2624, 2017.

KEY WORDS: HEAD AND NECK CANCER; PI3K/AKT SIGNALING PATHWAY; DOXORUBICIN; AD198

Oral squamous cell carcinoma (OSCC) is a major subset of head and neck cancers (HNC), which contribute to ~48,330 new cases a year in the United States, with a relatively low 5-year survival rate of only 63% [ACS, 2016]. OSCC arises from squamous epithelial cells and occurs most commonly in the individuals with the average age of diagnosis of 62 years old [OCF, 2015]. The most common risk factors of oral cancer are exposure to carcinogens (mainly tobacco use), alcohol consumption, and human papilloma virus (HPV), which is found in 40–60% of oral cancer patients [Furness et al., 2011]. Studies indicate that HPV-positive OSCC is more responsive to treatments and carries a better prognosis than HPV-negative OSCC [Benson et al., 2014]. The pathways that have been observed to be altered in HNC are the p63/NOTCH, TGFβ, and PI3K/AKT signaling pathways [Rothenberg and Ellisen, 2012].

Abbreviations: AD198, N-benzyladriamycin-14-valerate; AKT, protein kinase B; Dox, doxorubicin; ERK1/2, extracellular regulated kinases 1 and 2; H_2DCF-DA, dihydrogen-dichlorodihydro-fluorescein-diacetate; HNC, head and neck cancer; HPV, human papillomavirus; LY, LY294002 PI3 K inhibitor; MAPK, mitogen-activated protein kinase; OSCC, oral squamous cell carcinoma; PARP, poly (ADP-ribose) polymerase; PI3 K, phosphoinositide-3 kinase; ROS, reactive oxygen species.

Conflicts of interest: The authors declare no conflict of interest with the contents of this article.

Grant sponsor: National Institute of Health National Cancer Institute (NIH/NCI); Grant number: 1R15CA182850-01A1; Grant sponsor: University of Tennessee's Center of Excellence in Livestock Diseases and Human Health (UTCVM, COE); Grant number: R181721333; Grant sponsor: Milam's Foundation at the University of Tennessee College of Veterinary Medicine (UTCVM); Grant number: R181721152; Grant sponsor: Department of Small Animal Clinical Sciences at the College of Veterinary Medicine at the University of Tennessee (SACS, UTCVM); Grant number: E180120.

*Correspondence to: Maria Cekanova, RNDr, PhD, Department of Small Animal Clinical Sciences, College of Veterinary Medicine, The University of Tennessee, 2407 River Drive, RM A122, Knoxville 37996-4550, TN.
E-mail: mcekanov@utk.edu

Manuscript Received: 27 July 2016; Manuscript Accepted: 19 September 2016

Accepted manuscript online in Wiley Online Library (wileyonlinelibrary.com): 20 September 2016

DOI 10.1002/jcb.25747 • © 2016 Wiley Periodicals, Inc.

While the standard of care for patients with oral cancer is surgery, followed by radiation and chemotherapy, patients diagnosed with late stages very often cannot have a surgery due to the cancer's intensive spread [Furness et al., 2011]. Most common chemotherapy agents used for treatment of oral cancers include cisplatin, carboplatin, cetuximab, 5-flourouracil, docetaxel, paclitaxel, bleomycin, vinblastine, vincristine, and methotrexate [Furness et al., 2011]. Because chemotherapy for patients with unresectable tumors may prolong survival by 10–22%, there is a great need for more effective protocols and new drugs for treatment of OSCC [Furness et al., 2011]. Doxorubicin (Dox) has been used over the past 3 decades to treat solid metastatic tumors and is one of the most successful chemotherapeutic agents [Deavall et al., 2012]. Dox inhibits growth of cancerous cells by inducing DNA damage through type II topoisomerases and other mechanisms, including generation of reactive oxygen species within the cytoplasm [Bodley et al., 1989; Tsang et al., 2003]. Although, cisplatin and 5-fluorouracil-based chemotherapy are usually the first line of treatment for HNC, new formulations of Dox to target HNC are under investigation [Caponigro et al., 2000; Vermorken et al., 2007]. While Dox has been shown to be effective chemotherapy drug, its long-term use comes with the drawbacks of drug resistance and cumulative cardio-toxicity [Frishman et al., 1996]. A novel derivative of Dox, N-benzyladriamycin-14-valerate (AD198), has been specifically designed to address drug-resistance and cardio-toxicity in anthracycline-based therapies [Lothstein et al., 1992]. AD198 readily diffuses into the cytoplasm of the cell and is less susceptible to efflux transport due to its lipophilic structure [Lothstein et al., 2001]. Unlike Dox, AD198 not only has no detectable cardio-toxicity in the mouse and rat models, but AD198 has a cardio-protective effect through the activation of PKC-ε after Dox treatment [Cai et al., 2010].

Dogs and cats develop spontaneous cancers that are genetically more closely related to humans than mice that make them the valuable animal cancer models [Cekanova and Rathore, 2014]. HNC cancer accounts for 6% of all canine cancers and 10% of feline cancers reviewed in Cekanova and Rathore [2014]. Tobacco exposure has been linked to increased incidence of HNC in both human and pet populations, with cats having an increased incidence of OSCC and dogs having an increased incidence of nasal cancers [Lewin et al., 1998; Reif et al., 1998; DiBernardi et al., 2007]. As with humans, both canine and feline OSCC are locally invasive that cause difficulties for complete surgical resection reviewed in Cekanova and Rathore [2014].

Even Dox is not the first line of treatment in HNC cancers, strategies on how to increase its efficacy in this type of cancer should be further investigated. In this study, we evaluated the efficacy of Dox and its derivative AD198 on human OSCC and on primary canine and feline OSCC cells in vitro and elucidated a possible combined therapy approach that would make anthracycline therapy more effective in HNC.

MATERIALS AND METHODS

REAGENTS AND ANTIBODIES

Unless otherwise stated, all reagents and media were purchased from Fisher Scientific (Pittsburgh, PA). Dox and LY294002 (LY) were purchased from Sigma–Aldrich (St. Louis, MO). N-benzyladriamycin-14-valerate (AD198) was a kind gift from Dr. Leonard Lothstein, University of Tennessee Health Science Center in Memphis, TN [Lothstein et al., 1992]. The following antibodies were purchased from Santa Cruz Biotechnology (Santa Cruz, CA): Actin-HRP, p-ERK1/2, ERK1/2, AKT, and p38. The following antibodies were purchased from Cell Signaling (Boston, MA): PARP, p-AKT (Ser473 and Thr308), p-GSK3β, and p-p38.

CELL CULTURE

Human OSCC (SCC25) cells were purchased from ATCC (Manassas, VA). Human 1483 cells were kindly provided from Dr. Marnett's laboratory and originally developed by the Dr. Parson's laboratory [Sacks et al., 1988]. Canine and feline OSCC cell lines (K9OSCC-Abby and FeOSCC-Sidney, respectively) were established and characterized in Dr. Cekanova's laboratory [Rathore et al., 2014]. The SCC25 and 1483 cells were grown in the following media: DMEM/F-12 containing 10% FBS penicillin/streptomycin mixture at 37°C and 5% CO_2; feline and canine OSCC cells were grown in RPMI media containing 10% FBS and penicillin/streptomycin mixture (Fisher Scientific) at 37°C and 5% CO_2.

PROLIFERATION MTS ASSAY

Cells were plated in 96-well plates at 5×10^3 cells/well and allowed to attach for 24 h. After seeding, cells were treated with AD198 or Dox in a dose-dependent manner in complete media for an additional 48 h. DMSO was used as a control. For treatment with PI3K inhibitor, LY294002 (LY), cells were pretreated with 20 μM LY for 30 min prior to Dox or AD198 treatments, and 20 μM LY was maintained for the rest of the 48 h treatment. After treatment, cell proliferation was measured using CellTiter96® Aqueous One Solution Cell Proliferation Assay (Promega, Madison, WI) according to the manufacturer's protocol. Briefly, 20 μL MTS reagent was added to each well and allowed to incubate at 37°C for 1 h. Absorbance was measured at 490 nM using a plate reader (Bio-Tek instruments, Winooski, VT). The treatment data were normalized to the DMSO control.

ANNEXIN V-FITC DETECTION OF APOPTOSIS BY FLOW CYTOMETRY

SCC25 cells were plated in 6 cm petri dishes (PD) at density of 1×10^6 cells/PD. After 24 h, cells were treated with Dox (1 μM) and AD198 (1 μM) for an additional 24 h. DMSO, a vehicle for both treatment was used as a control. After treatment, both the media and attached cells were collected for analysis. Cells were stained with Annexin V-FITC and propidium iodide (PI) according to the TACS® Annexin V Kits protocol for apoptosis detection by flow cytometry (Trevigen, Inc. Gaithersburg, MD). The apoptotic cells were identified using a BD Biosciences Accuri C6 flow cytometer (San Jose, CA). Early apoptotic, late apoptotic, and necrotic cell counts were used for analysis.

REACTIVE OXYGEN SPECIES (ROS) ASSAY BY FLOW CYTOMETRY

For the ROS assay, the cells were incubated with 5 μM dihydrogen-dichlorodihydro-fluorescein-diacetate (H_2DCF-DA, Life Technologies, Grand Island, NY) for 1 h. Cells were then washed twice with PBS and trypsinized. The trypsin was neutralized and the collected

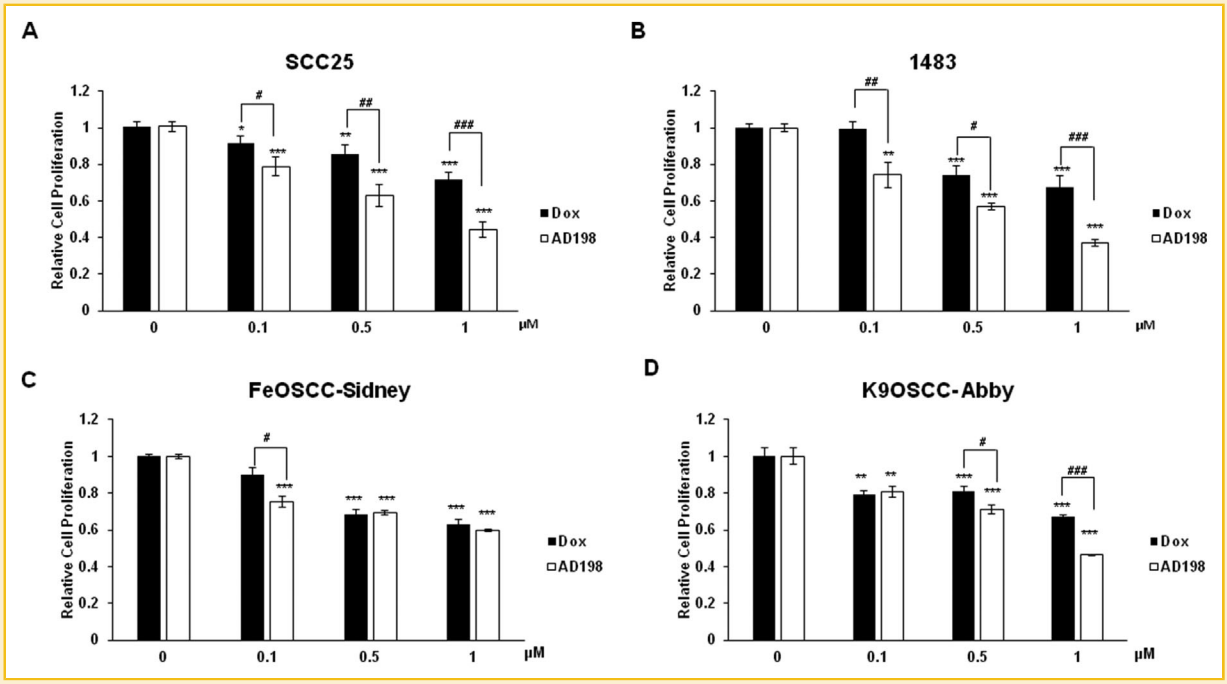

Fig. 1. Dox and AD198 inhibit cell viability of tested OSCC cells. (A) Human SCC25, (B) 1483 and feline, (C) FeOSCC-Sidney and canine, and (D) K9OSCC-Abby oral squamous cell carcinoma cells were treated with Dox (black bars) and AD198 (white bars) at 0, 0.1, 0.5, and 1 μM for 48 h. Cell proliferation was determined by MTS assay and relative cell growth rate was normalized to control, DMSO treated groups. The values are mean ± S.E. of four replicates from three independent experiments for SCC25 cells, four replicates from two independent experiments for 1483 cells and four replicates of one experiment for FeOSCC-Sidney and K9OSCC-Abby cells. Paired Student *t* tests were used to compare Dox and AD198 treatment to control; $^{*}P \leq 0.05$, $^{**}P \leq 0.01$, and $^{***}P \leq 0.001$. Paired Student *t* tests were used to compare among Dox and AD198 group at the same dose treatment; $^{\#}P \leq 0.05$, $^{\#\#}P \leq 0.01$, and $^{\#\#\#}P \leq 0.001$.

cells were centrifuged at 5,000 rpm for 5 min. The cell pellet was resuspended in 1 mL PBS and fluorescence signal was measured using a flow cytometer (ex 485 nm and em 530 nm, BD Accuri BD Sciences, San Jose, CA). Treatment results were normalized to the DMSO control.

CASPASE-3/7 ASSAY

Cells were plated in 6-well plates at 5×10^5 cells per well. After 24 h, cells were treated with AD198 or Dox for 24 h. After treatment, cells were washed twice with PBS, and cell lysates were harvested using RIPA buffer. Protein concentration was measured using a Bradford BCA assay. For detection of caspases 3/7, 40 μg proteins were used following the Caspase Glo-3/7 Substrate protocol (Promega). After 1 h incubation with reagents, luminescence was measured using an FLx800 plate reader (Bio-Tek instruments, Winooski, VT). The treatment data were normalized to the DMSO control.

WESTERN BLOT

Cells were plated at 1.5×10^6 cells per 10 cm plate. Twenty-four hours after plating, cells were treated with different doses of drugs for 24 h. For treatment with the PI3K inhibitor, LY294002, the cells were pretreated with 20 μM LY294002 for 30 min prior to Dox or AD198 treatments, and 20 μM LY294002 was maintained for the rest of the 24 h treatment. After treatment, the cells were washed twice with PBS and lysed using cold RIPA buffer containing protease/phosphatase inhibitors. The cell lysates were kept at −80°C until further analysis. Protein concentration was measured using the BCA protein assay. Equal amount of proteins (60 μg) were loaded onto SDS–PAGE gels and transferred to a nitrocellulose membrane. Primary antibodies were hybridized overnight at 4°C according to the manufacturer's instructions. The secondary antibodies were hybridized for 1 h at room temperature and the immunoreactive bands were visualized using enhanced chemiluminescence system (Fisher) and acquired on ImageQuant LAS4000 (GE Life Sciences, Pittsburgh, PA.) The densitometry analysis were performed using ImageJ (NIH, Bethesda, MD).

STATISTICAL ANALYSIS

Statistics were performed using a paired Student *t*-test to established significance. Results were considered statistically significant at $^{*}P \leq 0.05$, $^{**}P \leq 0.01$, $^{***}P \leq 0.001$ when treatments were compared to the control group and $^{\#}P \leq 0.05$, $^{\#\#}P \leq 0.01$, $^{\#\#\#}P \leq 0.001$ when comparing Dox to AD198, Dox to Dox + LY294002, or AD198 to AD198 + LY294002 at the same doses.

RESULTS

DOX AND AD198 INHIBITED VIABILITY OF HUMAN, CANINE, AND FELINE OSCC CELLS IN VITRO

The human OSCC cell lines, SCC25, and 1483, as well as FeOSCC-Sidney and K9OSCC-Abby cell lines, were treated with 0.1, 0.5, and

1 μM Dox and AD198 for 48 h, as shown in Figure 1. Both Dox and AD198 significantly reduced the proliferation of SCC25 (Fig. 1A) and 1483 (Fig. 1B) cells in a dose-dependent manner. AD198 was more effective at reducing cell viability at all doses when compared to Dox in human OSCC cells. Both Dox and AD198 inhibited viability of FeOSCC-Sidney (Fig. 1C) and K9OSCC-Abby (Fig. 1D) cells in a dose-dependent manner. AD198 was significantly more effective in inhibition of cell viability compared to Dox in FeOSCC-Sidney at 0.1 μM and significantly more effective than Dox in inhibition of cell viability in K9OSCC-Abby at 0.5 and 1 μM doses.

DOX AND AD198 INDUCED ROS PRODUCTION AND INDUCED APOPTOSIS THROUGH CASPASE ACTIVATION IN SCC25 CELLS

To evaluate the mechanisms of the anti-proliferative effects of Dox and AD198 in OSCC cells, we have used representative human SCC25 cell line for further experiments in this study.

After 24 h treatment, both Dox and AD198 increased apoptosis in SCC25 cells with a 4.2- and 15.8-fold increase, respectively, compared to control (DMSO) as shown in Figure 2A and Table I. AD198 increased the number of apoptotic cells as compared to Dox treatment. Both Dox and AD198 significantly increased ROS production in SCC25 cells after 24 h treatment with a 2.3- and 7.4-fold increase in SCC25 cells, respectively ($^{***}P \leq 0.001$), compared to control (Fig. 2B). In addition, AD198 showed significantly higher activation of ROS production as compared to Dox in SCC25 cells ($^{\#\#}P \leq 0.01$).

The effects of Dox and AD198 on induced apoptosis were evaluated using the caspase-3/7 activity assay. Dox increased caspase 3/7 activity by a 2.1-fold, and AD198 increased caspase activity by a 2.7-fold when compared to control ($^{***}P \leq 0.001$), but there was no significant difference between Dox and AD198 treatments (Fig. 2C). Poly (ADP-ribose) polymerase (PARP) is a downstream target of caspases cascade. PARP protein is cleaved by caspases and the presence of cleaved fragments indicates apoptosis [Duriez and Shah, 1997]. Dox and AD198 (1 μM) treatments increased the cleavage of PARP in SCC25 cells as confirmed by WB analysis (Fig. 2D). Densitometry values of cleaved PARP proteins after Dox and AD198 treatments were normalized to actin and then to the control groups, as shown in Figure 2D. According to densitometry analysis of three independent experiments, a statistically significant increase in PARP cleavage by 5.9-($^{*}P \leq 0.05$) and 4.7-fold ($^{**}P \leq 0.01$) was observed in Dox and

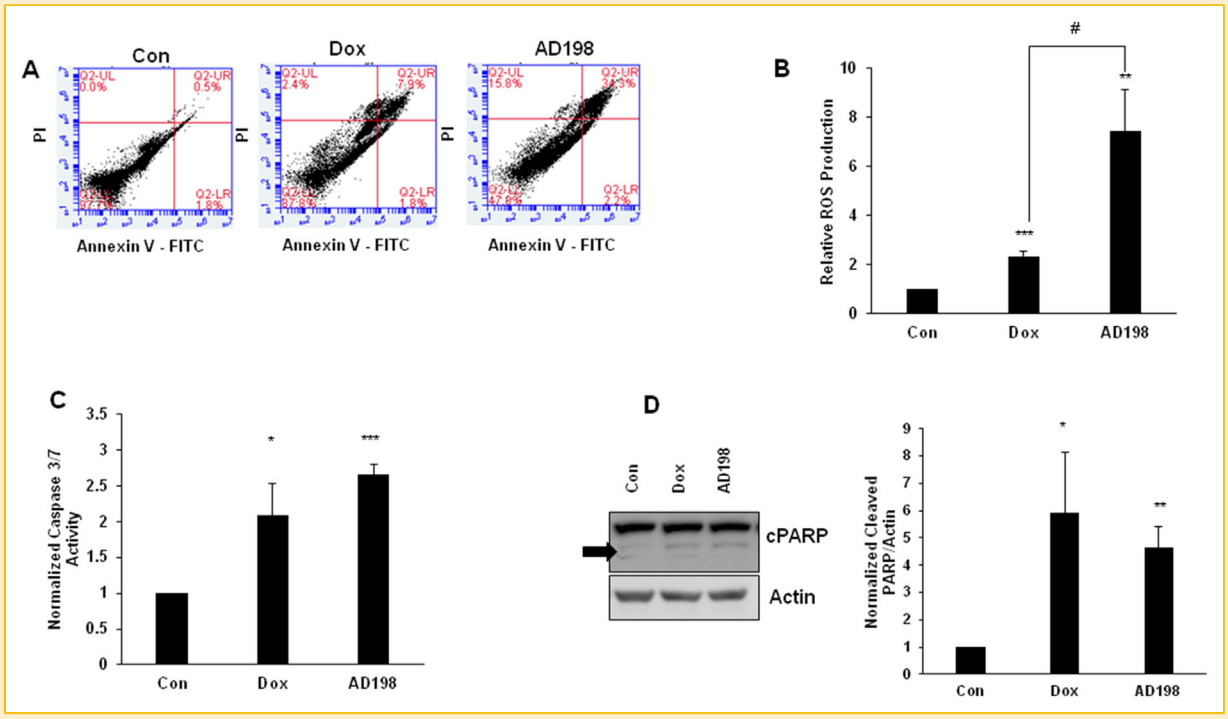

Fig. 2. Dox and AD198 induced apoptosis in human SCC25 cells and activated ROS and apoptotic caspase cascade. (A) SCC25 cells were treated with 1 μM Dox and 1 μM AD198 for 24 h, and apoptosis was measured by Annexin V–FITC and PI using flow cytometry assay. (B) SCC25 cells were treated with 1 μM Dox and 1 μM AD198 for 24 h, and ROS levels were measured with dihydrogen–dichlorodihydro–fluorescein–diacetate labeling flow cytometry; percent ROS positive cells were measured and normalized to the control. These values are mean ± S.E. of four replicates performed in two independent experiments. Paired Student *t*-test comparing Dox and AD198 treatment to control; $^{*}P \leq 0.05$, $^{***}P \leq 0.001$, and Dox and AD198 treatments; $^{\#\#}P \leq 0.01$, respectively. (C) SCC25 cells were treated with 1 μM Dox and 1 μM AD198 for 24 h, and caspase activity was measured using the Caspase–Glo 3/7 luminescence assay. Relative caspase activities were normalized to control. The values are mean ± S.E. of three independent experiments. Paired Student *t*-test compared treatment to control groups; $^{***}P \leq 0.001$. There was no significant difference in caspase activity between Dox and AD198. (D) SCC25 cells were treated with 1 μM Dox and 1 μM AD198 for 24 h. The expression of PARP (cleaved fragment) was evaluated by WB analysis. Actin was used as loading control. The right panel represents densitometry evaluation of three independent experiments. Cleaved PARP fragment was normalized to actin and these values were normalized to control. Values represent mean ± S.E. of three independent experiments. Paired Student *t*-test comparing Dox and AD198 treatment to control groups; $^{*}P \leq 0.05$ and $^{**}P \leq 0.01$.

TABLE I. Apoptosis Induced by Dox and AD198 in Human SCC25 Cells by Annexin V/PI Flow Cytometry

	Healthy cells (%)	Early apoptotic cells (%)	Late apoptotic cells (%)	Necrotic cells (%)	Normalized total apoptotic cells to control
Control (DMSO)	97.7	1.8	0.5	0	1.0
Doxorubicin (1 μM)	87.8	1.8	7.9	2.4	4.2
AD198 (1 μM)	47.8	2.2	34.3	15.8	15.9

AD198, respectively, as compared to control treatment. There was no significant difference in cleaved PARP between Dox and AD198 treatments.

DOX AND AD198 ACTIVATED THE PI3K/AKT SIGNALING PATHWAY IN SCC25 CELLS

To better understand the mechanisms of AD198 and Dox action on cell proliferation and apoptosis in OSCC, we investigated the role of PI3K/AKT and MAPKs signaling pathways. The p38 and ERK1/2 MAPKs have been shown to be activated by ROS to play vital role in apoptosis [Wold et al., 2005; Deng et al., 2010]. Both Dox and AD198 increased the phosphorylation of p38 and ERK1/2 MAPKs in a dose-dependent manner (Fig. 3A). Both Dox and AD198 increased phosphorylation of p38 MAPK in a time-dependent manner with the highest activation at 24 h after treatment (Fig. 3B). On the other hand, Dox and AD198 increased the pro-survival PI3K/AKT signaling pathway in SCC25 cells in dose- and time-dependent manners (Fig. 3A and B). Dox had the greatest effect of increasing phosphorylation of AKT protein at both Ser473 and Thr308 at the 1 μM dose, while AD198 had the greatest effect on the phosphorylation of AKT protein at 0.5 μM dose.

INHIBITION OF PI3K/AKT SIGNALING PATHWAY SENSITIZING THE CYTOTOXIC EFFECTS OF DOX AND AD198 IN SCC25 CELLS

Dox and AD198 activated the pro-survival PI3K/AKT signaling pathway, which is one of the indicators of resistance of cells to chemotherapy. To confirm our hypothesis, we tested the effects of the PI3K inhibitor, LY294002 (LY) in combination with Dox or AD198 on growth of SCC25 cells. Co-treatment with LY294002 increased the anti-proliferative effects of both Dox and AD198 in SCC25 cells. Cell morphology changes were detected, when cells were pre-treated with LY294002 and followed by Dox and AD198 treatments as compared to either Dox or AD198 treatments alone. Co-treatment of Dox with LY294002 caused cells to shrink and detach from plate surface resulting in cellular death of SCC25 cells (Fig. 4A.) The combination of Dox or AD198 and LY294002 more effectively suppressed cell viability of SCC25 cells as compared to either treatment alone (Fig. 4B).

In order to further investigate the PI3K/AKT inhibitor's chemo-sensitizing effect to Dox and AD198 chemotherapy, we measured caspase-3/7 activities and PARP cleavage. Co-treatment of Dox and AD198 with LY294002 increased caspase-3/7 activation and PARP cleavage in SCC25 cells, as shown in Figure 4C and D. LY294002

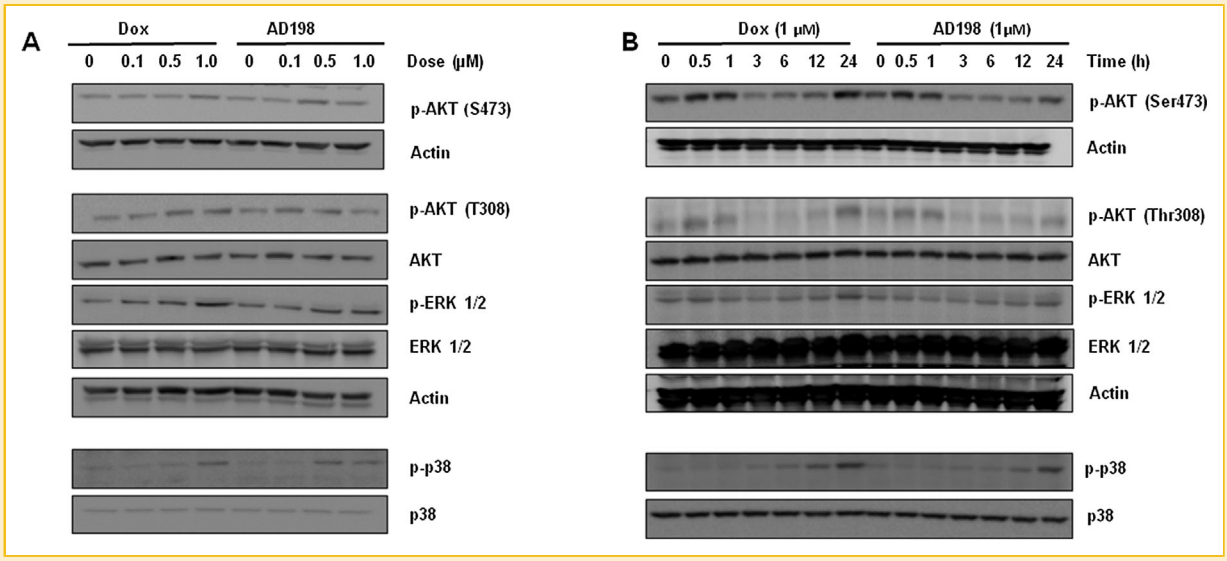

Fig. 3. Dox activated AKT, p38 MAPK, and ERK1/2 signaling pathways in human SCC25 cells in a dose- and time-dependent manners. (A) SCC25 cells were treated with 0, 0.1, 0.5, and 1 μM Dox and AD198 for 24 h. (B) SCC25 cells were treated with 1 μM Dox and 1 μM AD198 for 0, 0.5, 1, 3, 6, and 24 h. The expression of p-AKT (Thr308), p-AKT (Ser473), AKT, p-ERK1/2, ERK1/2, p-p38, and p38 proteins was detected by WB. Actin was used as loading control.

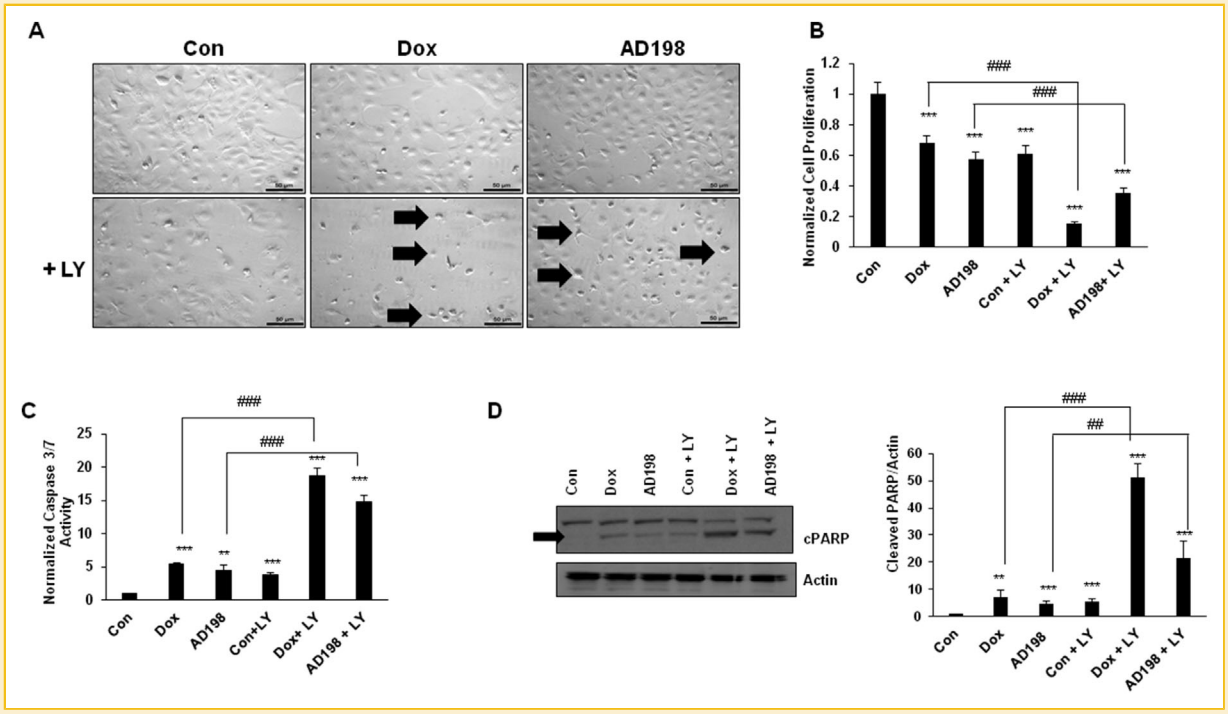

Fig. 4. Inhibition of the PI3K/AKT signaling pathway potentiates the cytotoxic effects of Dox in human SCC25 cells. (A) SCC25 cells were treated with Dox and AD198 (1 μM) with and without LY294002 (LY, 20 μM) for 24 h. Representative images of cells were taken at 100× magnification in order to observe cell morphology by a phase contrast microscope and captured by a MicroPublisher 3.3 camera (Q Imaging). Arrows indicate apoptotic cells. Scale bar represents 50 μm. (B) SCC25 cells were treated with Dox and AD198 (1 μM) with and without LY294002 (20 μM) for 48 h, and cell viability was measured using an MTS assay. Relative cell viability was normalized to untreated counterpart. The values represent mean ± S.E. of three independent experiments performed in four replicates. Paired Student *t* tests compared DOX, AD198, Dox + LY294002, and AD198 + LY294002 treatments to control; $^{***}P \leq 0.001$. Paired Student *t* tests were used to compare Dox to Dox + LY294002 and AD198 to AD198 + LY294002 treatments, $^{###}P \leq 0.001$. (C) SCC25 cells were treated with DOX and AD198 (1 μM) with and without LY294002 (20 μM) for 24 h, and caspase activities were measured using the Caspase-Glo 3/7 luminescence assay. Relative caspase activities were normalized to control. The values represent mean ± S.E. of two independent experiments performed in duplicates. A paired Student *t*-test compared treatment to control; $^{**}P \leq 0.01$, and $^{***}P \leq 0.001$, as well as Dox to Dox + LY294002 and AD198 to AD198 + LY294002 treatments; $^{###}P \leq 0.001$. (D) SCC25 cells were treated with Dox and AD198 (1 μM) with and without LY294002 (20 μM) for 24 h. The expression of PARP (cleaved fragment) was evaluated by WB analysis. Actin was used as loading control. Densitometry evaluation of cleaved PARP/actin protein bands from WB analysis was done using ImageJ software. Values are mean ± S.E. of measured densitometry of each protein's band from two independent experiments performed in duplicates. Paired Student *t* tests were used to compare Dox and AD198 treatments to control treatments, $^{**}P \leq 0.01$, and $^{***}P \leq 0.001$, as well as Dox to Dox + LY294002 and AD198 to AD198 + LY294002 treatments; $^{##}P \leq 0.01$, and $^{###}P \leq 0.001$.

inhibited the AD198- and Dox-induced phosphorylation of AKT Ser473 but not Thr308, as shown in Figure 5A and B. In addition, higher levels of active (unphosphorylated) GSK-3β were present when SCC25 cells were co-treated with Dox or AD198 with LY294002. Inhibition of PI3K/AKT further increased the Dox- and AD198-induced phosphorylation of p38 MAPK, but decreased the Dox- and AD198-induced phosphorylation of ERK1/2 Figure 5A and B.

DISCUSSION

AD198 is the effective derivative of Dox for treatment of Dox-resistance leukemia and melanoma tumors in the mouse model [Ganapathi et al., 1989]. The objectives of our study was to evaluate the efficacy of AD198 in human, canine, and feline OSCC cell lines in vitro. Our data showed that AD198 had a better inhibitory effects on cell proliferation than Dox in all tested human, canine and feline OSCC cell lines (Fig. 1). This data correlates with our previously obtained results that show that AD198 is more effective than Dox in inhibition of cell proliferation of primary canine transitional cell carcinoma and osteosarcoma cells in vitro [Rathore and Cekanova, 2015]. We and others have shown that feline and canine OSCC models might be helpful for testing of novel therapeutics, including Dox and its derivatives, receptor tyrosine kinase inhibitors, and non-steroidal anti-inflammatory drugs [DiBernardi et al., 2007; Rathore et al., 2014].

In order to elucidate mechanistic differences and potential ways to increase efficacy of Dox and AD198 chemotherapies, we studied the Dox and AD198-induced apoptosis in OSCC in vitro as shown in Figure 2A. While both Dox and AD198 increased apoptosis and ROS production when compared to control, AD198 increased ROS production by a 7.4-fold, Dox increased ROS production by only 2.3-fold ($^{##}P \leq 0.01$ between Dox and AD198, Fig. 2B). AD198 has been shown to have comparable ROS production with that of Dox in cardiomyocytes [Hofmann et al., 2007]. AD198 induces production

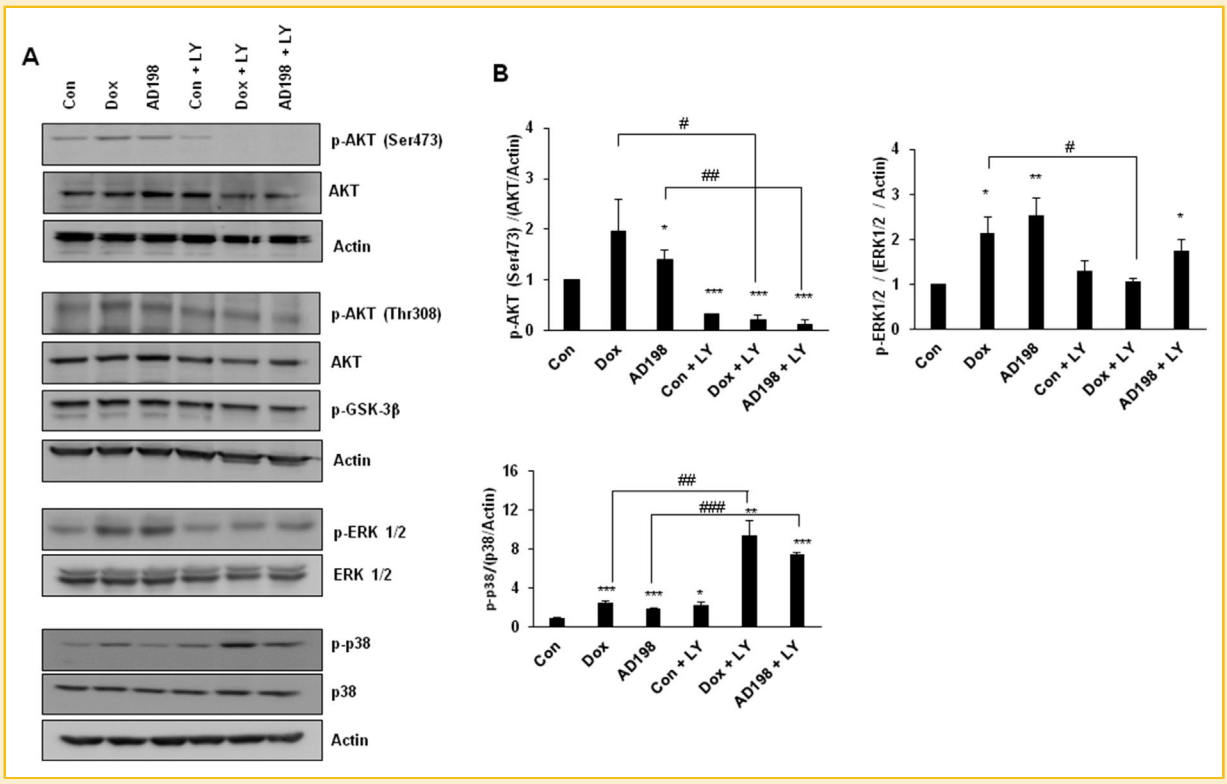

Fig. 5. Inhibition of the PI3K/AKT signaling pathway modulates ERK 1/2 and p38 MAPK signaling pathways. (A) SCC25 cells were treated with Dox and AD198 (1 μM) with and without LY294002 (20 μM) for 24 h. The expression of p-AKT (Thr308), p-AKT (Ser473), AKT, p-p38, p38, p-ERK1/2, ERK1/2, and p-GSK-3β proteins was evaluated by WB analysis. Actin was used as loading control. (B) Densitometry analysis of combination treatment of LY294002 combined with Dox or AD198 on the phosphorylation status of AKT (Ser473), p38 MAPK, and ERK1/2. The intensity of phosphorylated protein was normalized to total levels of protein/actin which was then normalized to the DMSO control. Values are mean ± S.E of three independent experiments. Paired Student *t* tests were used to compare Dox and AD198 treatments to control treatments, $^{*}P \leq 0.05$, $^{**}P \leq 0.01$, and $^{***}P \leq 0.001$, as well as Dox to Dox + LY294002 and AD198 to AD198 + LY294002 treatments; $^{\#\#\#}P \leq 0.05$, $^{\#\#\#}P \leq 0.01$, and $^{\#\#\#}P \leq 0.001$.

of ROS more than Dox in human UMUC3 and T24 bladder cancer cells in vitro [Smolensky et al., 2015]. Caspase cascade and its downstream target PARP cleavage are common methods to detect apoptosis in cells [Duriez and Shah, 1997]. Both Dox and AD198 had similar effects in increasing caspase 3/7 activities and inducing downstream PARP cleavage in tested OSCC cells in vitro (Fig. 2C and D). There was no significant difference in caspase 3/7 activities with regard to the amount of cleaved PARP between Dox and AD198 in tested OSCC cells. These data suggest that while AD198 has a greater ROS-generating effect, this effect may not contribute to an increase in caspase-dependent apoptosis, but instead may to contribute to caspase-independent pathways. Dox-induced apoptosis is caspase-dependent, and its diminish when caspases are inhibited in leukemia cells [Gamen et al., 1997]. In addition, ROS-induced apoptosis can function through caspase-independent pathways, as shown previously in cardiomyocytes [Bernuzzi et al., 2009]. This suggests that the greater increase in ROS production may still lead to greater apoptosis without triggering a great increase in caspase activity.

To further investigate the mechanism behind Dox and AD198 anti-tumor effects, we evaluated the involvement of signal transduction pathways in tested OSCC cells in vitro. Both Dox and AD198 increased phosphorylation of ERK1/2, and p38 MAPK, as well as AKT in time- and dose-dependent manners (Fig. 3A and B). The ERK1/2 signaling pathway plays an important role in regulation of cell's survival and apoptosis [Boucher et al., 2000; Tran et al., 2001]. Activation of ERK1/2 generally promotes cell survival; but can also have pro-apoptotic functions [Wang et al., 2000; Lu and Xu, 2006]. The inhibition of ERK2 activity has been reported to sensitize ovarian carcinoma cells to cisplatin-induced apoptosis [Hayakawa et al., 1999; Persons et al., 2000], but it has been also reported to induced drug resistance of various carcinomas to chemotherapy drugs [Yeh et al., 2002, 2004]. The p38 MAPK signaling pathway is also associated with apoptosis and is an important pathway that is activated with various chemotherapy drugs [Olson and Hallahan, 2004]. Dox- and AD198-induced apoptosis is a p38 MAPK-dependent in canine transitional cell carcinoma and osteosarcoma cells [Rathore and Cekanova, 2015].

PI3K/AKT pathway has been shown to be dysregulated in many cancers, and its activation is responsible for increased cell survival, decreased apoptosis, and increased drug resistance [West et al., 2002; Osaki et al., 2004]. In breast cancer, activation of AKT leads to

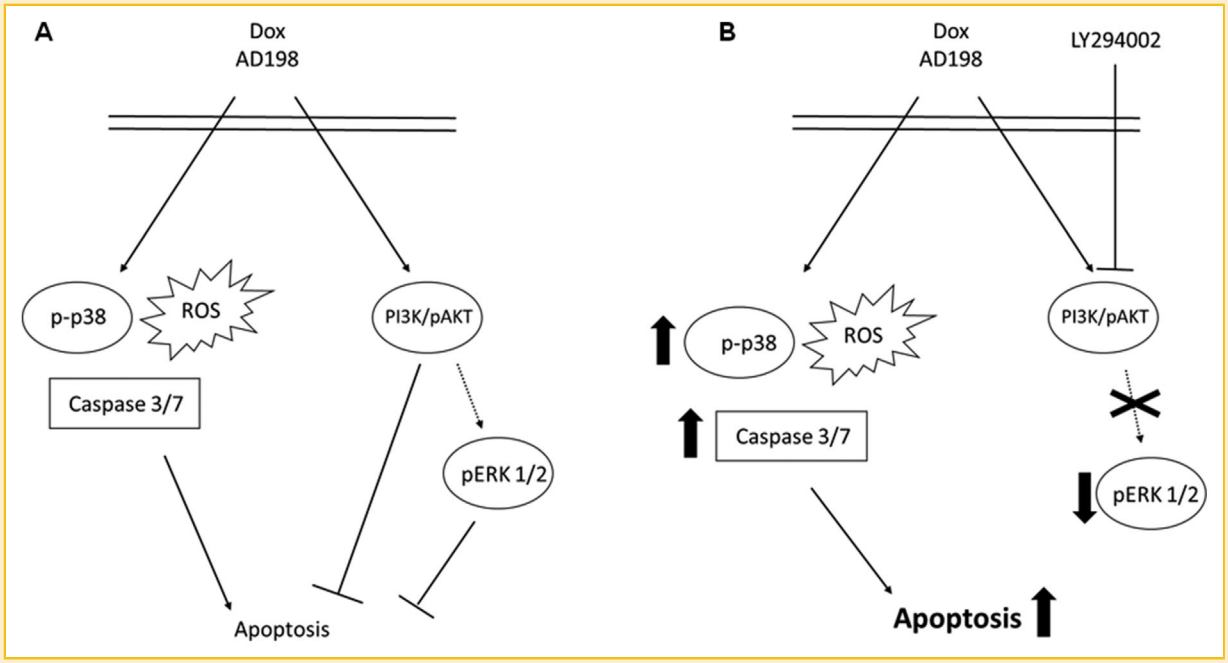

Fig. 6. Schematic representation of Dox- and AD198-induced apoptosis and chemosensitization by inhibition of the PI3K/AKT pathway with LY294002 in OSCCs in vitro. (A) Dox and AD198 treatments of SCC25 cells induced apoptosis through the generation of ROS, activation of the p38 MAPK pathway, and downstream activation of the caspase 3/7 apoptotic pathway. Dox and AD198 increased the activity of PI3K/AKT signaling pathway and ERK1/2 signaling pathway. (B) Upon inhibition of PI3K, neither Dox nor AD198 induced phosphorylation of AKT (Ser473) or ERK1/2. Inhibition of PI3K/AKT induced a greater anti-proliferative effect of Dox or AD198 by further increasing the p38 MAPK pathway and the caspase 3/7 apoptotic pathway.

multi-drug resistance and increased expression of p-glycoprotein [Knuefermann et al., 2003]. In contrast, inhibition of PI3K/AKT reduces drug resistance by decreasing transport activity of p-glycoprotein [Barančík et al., 2006]. When the PI3K/AKT pathway is inhibited, chemosensitivity to Dox is increased in various cancers, including ovarian, and bladder [Wu et al., 2011; Bezler et al., 2012], which correlates with our observations in SCC25 cells. In order to better understand how activation of PI3K/AKT pathway plays a role in antagonizing Dox and AD198-induced apoptosis in OSCC cells, we studied the effects of Dox and AD198 in combination with the PI3K inhibitor LY294002. Cell viability of tested OSCC was greatly reduced when Dox or AD198 was combined with LY294002 treatment when compared to either Dox or AD198 treatment alone (Fig. 4A and B). Apoptotic markers, including caspase 3/7 activity and PARP cleavage, increased significantly with the combination of Dox + LY294002 or AD198 + LY294002, as compared to either Dox or AD198 alone (Fig. 4C and D). Our results also show that chemosensitivity to AD198 can also be increased through the inhibition of the PI3K/AKT pathway.

Inhibition of the PI3K/AKT signaling pathway decreased Dox- and AD198-induced activation of p38 MAPK and reduced activation of the ERK1/2 signaling pathways (Fig. 5A and B). It has been previously shown that ROS activates both AKT and ERK1/2 signaling pathways and increases proliferation in hepatoma cell lines [Liu et al., 2002]. ROS activates AKT that is is modulated by LY294002 [Liu et al., 2002]. In cardiomyocytes, activation of AKT is correlated with deactivation of p38 MAPK [Das et al., 2011]. PI3K/AKT signaling pathway has also been shown to downregulate p38 MAPK signaling in endothelial cells [Gratton et al., 2001]. While the interaction between PI3K/AKT and ERK signaling pathways is poorly understood, it has been previously observed that inhibition of the ERK signaling pathway increases activity of the p38 MAPK pathway [Berra et al., 1998]. In breast cancer, PI3K has been shown to regulate the ERK1/2 signaling pathway through the phosphorylation of Rac protein which is downstream of RAS [Ebi et al., 2013]. The inhibition of PI3K has been shown to induce apoptosis through the inhibition of ERK1/2 activity [Will et al., 2014]. Our results indicate that LY294002 co-treatment with Dox or AD198 increased chemosensitivity through the inhibition of PI3K/AKT signaling pathway as well as the ERK1/2 signaling pathway and increased activation of p38 MAPK (Fig. 6). In conclusion, our data show that the inhibition of the PI3K pathway may be an important for increasing the efficacy of anthracycline-based chemotherapy in HNC with agents such as Dox and AD198.

CONCLUSION

In this study, we have shown that AD198 is more effective in inhibiting cell proliferation than Dox in tested OSCC cell lines. Both Dox and AD198 increased ROS production and activated the caspase-dependent apoptosis cascade. Phosphorylation of AKT, p38 MAPK, and ERK1/2 was increased by both Dox and AD198 treatments. Because AKT was shown to have an anti-apoptotic

effect in previous studies, we evaluated the combination therapy of inhibiting PI3K/AKT along with Dox and AD198. Inhibition of PI3K/AKT further decreased cell proliferation and increased apoptosis in human OSCC cells that were treated with Dox or AD198. Furthermore, inhibition of PI3K/AKT increased the activation of p38 MAPK by Dox and AD198 while decreasing the activation of ERK 1/2. Results collected from this study show that AD198 may be an effective anthracycline treatment for HNC cancers, and the inhibition of PI3K/AKT can further increase the efficacy of Dox or AD198-based chemotherapy in HNC cancers in vitro.

AUTHORS' CONTRIBUTION

MC conceived, coordinated the study, wrote the manuscript, and obtained funding for this study. DS, KR, and JB collected the data, analyzed the data of proliferation, apoptosis and WB analysis, and wrote the manuscript. All authors reviewed and approved the manuscript.

ACKNOWLEDGMENTS

This work was supported in part by the National Institute of Health National Cancer Institute (NIH/NCI) Grant ID: 1R15CA182850-01A1 (to MC); by the University of Tennessee's Center of Excellence in Livestock Diseases and Human Health (UTCVM, COE) Grant ID: R181721333 (to MC); Milam's Foundation at the University of Tennessee College of Veterinary Medicine (UTCVM) Grant ID: R181721152 (to MC); and used the resources of the Department of Small Animal Clinical Sciences at the College of Veterinary Medicine at the University of Tennessee (SACS, UTCVM) Grant ID: E180120 (to MC).

REFERENCES

ACS. 2016. Cancer Facts and Figures. American Cancer Society.

Barančík M, Boháčová V, Sedlák J, Sulová Z, Breier A. 2006. LY294, 002, a specific inhibitor of PI3 K/Akt kinase pathway, antagonizes P-glycoprotein-mediated multidrug resistance. Eur J Pharm Sci 29:426–434.

Benson E, Li R, Eisele D, Fakhry C. 2014. The clinical impact of HPV tumor status upon head and neck squamous cell carcinomas. Oral Oncol 50:565–574.

Bernuzzi F, Recalcati S, Alberghini A, Cairo G. 2009. Reactive oxygen species-independent apoptosis in doxorubicin-treated H9c2 cardiomyocytes: Role for heme oxygenase-1 down-modulation. Chem Biol Interact 177: 12–20.

Berra E, Diaz-Meco MaT, Moscat J. 1998. The activation of p38 and apoptosis by the inhibition of Erk is antagonized by the phosphoinositide 3-kinase/Akt pathway. J Biol Chem 273:10792–10797.

Bezler M, Hengstler JG, Ullrich A. 2012. Inhibition of doxorubicin-induced HER3-PI3K-AKT signalling enhances apoptosis of ovarian cancer cells. Mol Oncol 6:516–529.

Bodley A, Liu LF, Israel M, Seshadri R, Koseki Y, Giuliani FC, Kirschenbaum S, Silber R, Potmesil M. 1989. DNA topoisomerase II-mediated interaction of doxorubicin and daunorubicin congeners with DNA. Cancer Res 49:5969–5978.

Boucher MJ, Morisset J, Vachon PH, Reed JC, Lainé J, Rivard N. 2000. MEK/ERK signaling pathway regulates the expression of Bcl-2, Bcl-XL, and Mcl-1 and promotes survival of human pancreatic cancer cells. J Cell Biochem 79:355–369.

Cai C, Lothstein L, Morrison RR, Hofmann PA. 2010. Protection from doxorubicin-induced cardiomyopathy using the modified anthracycline N-benzyladriamycin-14-valerate (AD 198). J Pharmacol Exp Ther 335:223–230.

Caponigro F, Cornelia P, Budillon A, Bryce J, Avallone A, De Rosa V, Ionna F, Cornelia G. 2000. Phase I study of Caelyx (doxorubicin HCL, pegylated liposomal) in recurrent or metastatic head and neck cancer. Ann Oncol 11:339–342.

Cekanova M, Rathore K. 2014. Animal models and therapeutic molecular targets of cancer: Utility and limitations. Drug Des Devel Ther 8:1911.

Das J, Ghosh J, Manna P, Sil PC. 2011. Taurine suppresses doxorubicin-triggered oxidative stress and cardiac apoptosis in rat via up-regulation of PI3-K/Akt and inhibition of p53, p38-JNK. Biochem Pharmacol 81:891–909.

Deavall DG, Martin EA, Horner JM, Roberts R. 2012. Drug-induced oxidative stress and toxicity. J Toxicol 2012:645460.

Deng YT, Huang HC, Lin JK. 2010. Rotenone induces apoptosis in MCF-7 human breast cancer cell-mediated ROS through JNK and p38 signaling. Mol Carcinog 49:141–151.

DiBernardi L, Doré M, Davis JA, Owens JG, Mohammed SI, Guptill CF, Knapp DW. 2007. Study of feline oral squamous cell carcinoma: Potential target for cyclooxygenase inhibitor treatment. Prostaglandins Leukot Essent Fatty Acids 76:245–250.

Duriez PJ, Shah GM. 1997. Cleavage of poly(ADP-ribose) polymerase: A sensitive parameter to study cell death. Biochem Cell Biol 75:337–349.

Ebi H, Costa C, Faber AC, Nishtala M, Kotani H, Juric D, Della Pelle P, Song Y, Yano S, Mino-Kenudson M, Benes CH, Engelman JA. 2013. PI3 K regulates MEK/ERK signaling in breast cancer via the Rac-GEF, P-Rex1. Proc Natl Acad Sci USA 110:21124–21129.

Frishman WH, Sung HM, Yee HCM, Liu LL, Einzig AI, Dutcher J, Keefe D. 1996. Cardiovascular toxicity with cancer chemotherapy. Curr Probl Cardiol 21:227–286.

Furness S, Glenny AM, Worthington HV, Pavitt S, Oliver R, Clarkson JE, Macluskey M, Chan KK, Conway DI. 2011. Interventions for the treatment of oral cavity and oropharyngeal cancer: Chemotherapy. Cochrane Database Syst Rev 4:Cd006386. doi: 10.1002/14651858.CD006386.pub3. PMID: 21491393

Gamen S, Anel A, Lasierra P, MaA Alava, Martinez-Lorenzo MJ, Piñeiro A, Naval J. 1997. Doxorubicin-induced apoptosis in human T-cell leukemia is mediated by caspase-3 activation in a Fas-independent way. FEBS Lett 417:360–364.

Ganapathi R, Grabowski D, Sweatman TW, Seshadri R, Israel M. 1989. N-benzyladriamycin-14-valerate versus progressively doxorubicin-resistant murine tumours: Cellular pharmacology and characterisation of cross-resistance in vitro and in vivo. Br J Cancer 60:819–826.

Gratton J-P, Morales-Ruiz M, Kureishi Y, Fulton D, Walsh K, Sessa WC. 2001. Akt down-regulation of p38 signaling provides a novel mechanism of vascular endothelial growth factor-mediated cytoprotection in endothelial cells. J Biol Chem 276:30359–30365.

Hayakawa J, Ohmichi M, Kurachi H, Ikegami H, Kimura A, Matsuoka T, Jikihara H, Mercola D, Murata Y. 1999. Inhibition of extracellular signal-regulated protein kinase or c-Jun N-terminal protein kinase cascade, differentially activated by cisplatin, sensitizes human ovarian cancer cell line. J Biolo Chem 274:31648–31654.

Hofmann PA, Israel M, Koseki Y, Laskin J, Gray J, Janik A, Sweatman TW, Lothstein L. 2007. N-benzyladriamycin-14-valerate (AD 198): A non-cardiotoxic anthracycline that is cardioprotective through PKC-ϵ activation. J Pharmacol Exp Ther 323:658–664.

Knuefermann C, Lu Y, Liu B, Jin W, Liang K, Wu L, Schmidt M, Mills GB, Mendelsohn J, Fan Z. 2003. HER2/PI-3K/Akt activation leads to a multidrug resistance in human breast adenocarcinoma cells. Oncogene 22:3205–3212.

Lewin F, Norell SE, Johansson H, Gustavsson P, Wennerberg J, Biörklund A, Rutqvist LE. 1998. Smoking tobacco, oral snuff, and alcohol in the etiology of squamous cell carcinoma of the head and neck. Cancer 82:1367–1375.

Liu SL, Lin X, Shi DY, Cheng J, Wu CQ, Zhang YD. 2002. Reactive oxygen species stimulated human hepatoma cell proliferation via cross-talk between PI3-K/PKB and JNK signaling pathways. Arch Biochem Biophys 406:173–182.

Lothstein L, Israel M, Sweatman TW. 2001. Anthracycline drug targeting: Cytoplasmic versus nuclear-a fork in the road. Drug Resist Updat 4:169–177.

Lothstein L, Wright HM, Sweatman TW, Israel M. 1992. N-benzyladriamycin-14-valerate and drug resistance: Correlation of anthracycline structural modification with intracellular accumulation and distribution in multidrug resistant cells. Oncol Res 4:341–347.

Lu Z, Xu S. 2006. ERK1/2 MAP kinases in cell survival and apoptosis. IUBMB Life 58:621–631.

OCF. 2015. Oral Cancer Facts. Editors: Oral Cancer Foundation.

Olson JM, Hallahan AR. 2004. P38 MAP kinase: A convergence point in cancer therapy. Trends Mol Med 10:125–129.

Osaki M, Ma Oshimura, Ito H. 2004. PI3K-Akt pathway: Its functions and alterations in human cancer. Apoptosis 9:667–676.

Persons DL, Yazlovitskaya EM, Pelling JC. 2000. Effect of extracellular signal-regulated kinase on p53 accumulation in response to cisplatin. J Biol Chem 275:35778–35785.

Rathore K, Alexander M, Cekanova M. 2014. Piroxicam inhibits Masitinib-induced cyclooxygenase 2 expression in oral squamous cell carcinoma cells in vitro. Transl Res 164:158–168.

Rathore K, Cekanova M. 2015. A novel derivative of doxorubicin, AD198, inhibits canine transitional cell carcinoma and osteosarcoma cells in vitro. Drug Des Devel Ther 2015:5323–5335.

Reif JS, Bruns C, Lower KS. 1998. Cancer of the nasal cavity and paranasal sinuses and exposure to environmental tobacco smoke in pet dogs. Am J Epidemiol 147:488–492.

Rothenberg SM, Ellisen LW. 2012. The molecular pathogenesis of head and neck squamous cell carcinoma. J Clin Invest 122:1951–1957.

Sacks PG, Parnes SM, Gallick GE, Mansouri Z, Lichtner R, Satya-Prakash KL, Pathak S, Parsons DF. 1988. Establishment and characterization of two new squamous cell carcinoma cell lines derived from tumors of the head and neck. Cancer Res 48:2858–2866.

Smolensky D, Rathore K, Cekanova M. 2015. Phosphatidylinositol-3-kinase inhibitor induces chemosensitivity to a novel derivative of doxorubicin, AD198 chemotherapy in human bladder cancer cells in vitro. BMC Cancer 15:1.

Tran SE, Holmström TH, Ahonen M, Kähäri V-M, Eriksson JE. 2001. MAPK/ERK overrides the apoptotic signaling from Fas, TNF, and TRAIL receptors. J Biol Chem 276:16484–16490.

Tsang WP, Chau SPY, Kong SK, Fung KP, Kwok TT. 2003. Reactive oxygen species mediate doxorubicin induced p53-independent apoptosis. Life Sci 73:2047–2058.

Vermorken JB, Remenar E, Van Herpen C, Gorlia T, Mesia R, Degardin M, Stewart JS, Jelic S, Betka J, Preiss JH. 2007. Cisplatin, fluorouracil, and docetaxel in unresectable head and neck cancer. N Engl J Med 357:1695–1704.

Wang X, Martindale JL, Holbrook NJ. 2000. Requirement for ERK activation in cisplatin-induced apoptosis. J Biol Chem 275:39435–39443.

West KA, Castillo SS, Dennis PA. 2002. Activation of the PI3K/Akt pathway and chemotherapeutic resistance. Drug Resist Updat 5:234–248.

Will M, Qin ACR, Toy W, Yao Z, Rodrik-Outmezguine V, Schneider C, Huang X, Monian P, Jiang X, De Stanchina E. 2014. Rapid induction of apoptosis by PI3K inhibitors is dependent upon their transient inhibition of RAS-ERK signaling. Cancer Discov 4:334–347.

Wold LE, Aberle NS, Ren J. 2005. Doxorubicin induces cardiomyocyte dysfunction via a p38 MAP kinase-dependent oxidative stress mechanism. Cancer Detect Prev 29:294–299.

Wu D, Tao J, Xu B, Qing W, Li P, Lu Q, Zhang W. 2011. Phosphatidylinositol 3-kinase inhibitor LY294002 suppresses proliferation and sensitizes doxorubicin chemotherapy in bladder cancer cells. Urol Int 87:105–113.

Yeh PY, Chuang S-E, Yeh K-H, Song YC, Chang LL-Y, Cheng A-L. 2004. Phosphorylation of p53 on Thr55 by ERK2 is necessary for doxorubicin-induced p53 activation and cell death. Oncogene 23:3580–3588.

Yeh PY, Chuang S-E, Yeh K-H, Song YC, Ea C-K, Cheng A-L. 2002. Increase of the resistance of human cervical carcinoma cells to cisplatin by inhibition of the MEK to ERK signaling pathway partly via enhancement of anticancer drug-induced NFκB activation. Biochem Pharmacol 63:1423–1430.